electronics

MDPI

Article

Research on Reactive Power Coordination Control Strategies of Multi-Infeed Line-Commutated Converter–High-Voltage Direct Current Systems

Yueyang Yin [1], Ying Huang [1,*], Zheren Zhang [1], Guoteng Wang [1], Yijing Zhang [2] and Jianhua Li [2]

1 College of Electrical Engineering, Zhejiang University, Hangzhou 310027, China; 22110023@zju.edu.cn (Y.Y.); zhangzheren@zju.edu.cn (Z.Z.); wgt339@zju.edu.cn (G.W.)
2 East China Branch of State Grid Corporation of China, Shanghai 200120, China; zhang_yj@ec.sgcc.com.cn (Y.Z.); li_jianhua@ec.sgcc.com.cn (J.L.)
* Correspondence: huangyingzju@zju.edu.cn

Abstract: For a receiving-end power grid with multi-infeed LCC-HVDC systems, simultaneous commutation failures may seriously threaten the safe and stable operation of the system. To evaluate the impact of commutation failure and improve the voltage stability of the commutation buses in multi-infeed HVDC systems, this paper proposes a method for evaluating the voltage stability of commutation buses and a reactive power coordination control (RPCC) method for commutation failure of multiple HVDC systems. Firstly, three indicators and the entropy weight method are adopted to comprehensively evaluate the voltage stability of commutation buses. Then, an RPCC method is proposed to resist commutation failure. The proposed RPCC method uses the voltage interaction factor (VIF) to screen out DC systems that are strongly related to dynamic reactive power compensation devices and activates the devices to provide RPCC to the DC systems through an auxiliary controller. Finally, the effectiveness of the proposed method is verified through a practical example of the Jiangsu power grid.

Keywords: receiving-end power grid; commutation failure; comprehensive evaluation method; reactive power coordination control; line-commutated converter

check for updates

Citation: Yin, Y.; Huang, Y.; Zhang, Z.; Wang, G.; Zhang, Y.; Li, J. Research on Reactive Power Coordination Control Strategies of Multi-Infeed Line-Commutated Converter–High-Voltage Direct Current Systems. *Electronics* **2023**, *12*, 4262. https://doi.org/10.3390/electronics12204262

Academic Editor: Raffaele Giordano

Received: 16 August 2023
Revised: 21 September 2023
Accepted: 12 October 2023
Published: 15 October 2023

1. Introduction

With the implementation of the West to East Power Transmission Project, the number and capacity of HVDC systems have significantly increased, and the power grid on the eastern coast of China has gradually evolved into a receiving-end power grid with high DC power penetration [1]. Due to the commutation failure of inverter side line-commutated converters (LCCs) [2], the simultaneous commutation failure of multiple HVDC systems has become one of the important factors threatening the safe and stable operation of receiving-end power grids [3]. The simultaneous commutation failure of multiple HVDC systems can lead to short-term power shortages in the system, disrupt the power supply and demand balance, and even cause system instability. To ensure the safe and stable operation of the receiving-end power grid with high DC power penetration, it is urgent to study a method for evaluating the voltage stability of commutation buses and a reactive power coordination control (RPCC) method for commutation failure of multiple HVDC systems.

For the evaluation of the voltage stability of commutation buses in multi-infeed HVDC systems, the commonly used method in engineering is to use the short-circuit ratio (SCR) [4]. The SCR itself is an evaluation indicator that measures the relative strength between AC and DC systems, directly reflecting the static stability of HVDC systems. There is not a rigorous mathematical relationship between SCR and transient stability problems, such as commutation failure. However, better static stability usually means better transient stability, which means HVDC systems can quickly recover from a commutation failure.

Therefore, SCR remains an important tool in the evaluation of the voltage stability of commutation buses, and various indicators, such as generalized short-circuit ratio [5] and integrated short-circuit ratio [6], have been derived from this indicator. Many factors cause commutation failure in DC systems, including AC voltage drop, DC current sudden change, and harmonics [7]. According to different causes of commutation failure, scholars have conducted a large number of risk assessment studies on commutation failure. The authors of [8] constructed a risk assessment index system for commutation failure based on the voltage–time area (VTA) method. The authors of [9,10] proposed a voltage coupling factor for AC-DC systems to evaluate the risk of commutation failure in multi-infeed HVDC systems. The above studies are all aimed at evaluating the risk of commutation failure in HVDC systems under AC power grid faults. In addition, the risk assessment of commutation failure caused by asymmetric faults [11], non-characteristic harmonics [12], inrush current [13], and harmonic voltage [14] has also been thoroughly studied. However, the current assessment of commutation failure mainly focuses on the risk assessment of commutation failure and how to detect commutation failure [15,16]. Generally speaking, commutation failure is unavoidable, but it can be prevented from causing serious harm to the power system through reasonable planning and control methods. Evaluating the voltage stability of commutation buses can help operators determine whether the current planning and control scheme is reasonable. Therefore, the evaluation method for voltage stability of commutation buses in multi-infeed HVDC systems considering the severity of commutation failure needs further research. To address the above issues, this paper proposes a method for evaluating the voltage stability of commutation buses for commutation failure of multiple HVDC systems. The evaluation method for voltage stability of commutation buses in multi-infeed HVDC systems consists of two parts: one is the evaluation indicator system for voltage stability of commutation buses, and the other is a comprehensive evaluation method based on the entropy weight method.

Currently, the measures to resist the commutation failure are mainly from three perspectives: one is to use reactive power compensation devices to maintain the stability of commutation voltage, the second is to limit the rise of DC current, and the third is to increase the setting value of the turn-off angle [17,18]. The latter two measures are based on the control of LCC, which has limited improvement effect and is not beneficial to the economic operation of the DC system [19]. In this paper, we mainly consider resisting the problem of multiple HVDC commutation failures from the perspective of dynamic reactive power compensation, improving the security and stability of receiving-end power grids with high DC power penetration. The authors of [20,21] and [22], respectively, introduced the effectiveness of synchronous condensers and power electronic devices in supporting multi-infeed power grids and pointed out that dynamic reactive power compensation devices can effectively solve the threat of commutation failure.

In order to address the threat of commutation failure and minimize construction costs, scholars have conducted extensive research on the optimization configuration of dynamic reactive power compensation devices. The authors of [23] proposed an optimal configuration scheme for dynamic reactive power compensation devices to suppress the risk of subsequent commutation failure. The authors of [24] proposed a reliable and applicable site selection scheme for synchronous condensers to restrain commutation failures of multi-infeed HVDC systems. The authors of [25] pointed out that the dynamic reactive power compensation device can improve the recovery speed of multi-infeed HVDC systems, and a reactive power compensation site selection scheme is provided. Most existing studies focus on optimizing the configuration of reactive power compensation devices, but dynamic reactive power compensation devices usually take local signals as the control objective, which makes it difficult to fully utilize dynamic reactive power compensation devices with conventional control strategies. Therefore, control methods that can fully exploit the voltage support capability of dynamic reactive power compensation devices for DC systems need further research. To address the above issues, this paper proposes an RPCC method for the commutation failure of multiple HVDC systems. The RPCC method first determines the degree of influence between the dynamic reactive power compensation device that already exists and the DC system, filtering the DC system that is greatly affected by the dynamic reactive power compensation device, and then providing an auxiliary control strategy to make the dynamic reactive power compensation device fully utilize its capability to resist the commutation failure of the DC system.

The remainder of this article is organized as follows. In Section 2, the evaluation method for the voltage stability of commutation buses in multi-infeed HVDC systems is further clarified. In Section 3, the RPCC method based on a dynamic reactive power compensation device is developed. Section 4 verifies the effectiveness of the methods proposed in Sections 2 and 3. Finally, Section 5 concludes this article.

2. Evaluation Method for the Voltage Stability of Commutation Buses in Multi-Infeed HVDC Systems

For a multi-infeed receiving-end power grid, the simultaneous commutation failure of multiple HVDC systems can seriously threaten its safe and stable operation. If the power grid is weak, the voltage support capability of the AC system to the conventional DC inverter station is insufficient, and it is difficult to recover from the HVDC commutation failure; the power grid will face the risk of a power outage. If the power grid is too strong, the short-circuit current will have the risk of exceeding the limits, and because the coupling degree between individual DCs is relatively high, the risk of simultaneous commutation failure increases. Therefore, the evaluation of the voltage stability of commutation buses in multi-infeed HVDC systems is an important prerequisite to ensure the safe and stable operation of these systems. In the following, the corresponding evaluation indicators are provided according to the characteristics of the receiving-end grid with a multi-infeed HVDC.

2.1. Proportion of Short-Circuit Faults Causing DC Commutation Failure

If a bus causes a commutation failure in a conventional DC system at the moment of a three-phase grounded short-circuit fault, then the bus is considered to be the commutation failure-related bus of the DC system. The ratio of all commutation failure-related buses of a DC system to the total number of buses of the power grid is considered the proportion of commutation failure of the DC system due to a three-phase grounded short-circuit fault and is used as an indicator to evaluate the adaptability of the receiving-end grid to the DC system. The value of this indicator can be used to measure the fault occurrence range of DC system commutation failure caused by a short-circuit fault; the larger the value of the indicator, the larger the fault range and the more likely the DC system will suffer from commutation failure, which can reflect the adaptability of the AC system grid structure to the DC system. The indicator is shown as follows:

$$K_{\mathrm{fail}} = \frac{n_{\mathrm{fail}}}{N_{\mathrm{sum}}} \tag{1}$$

where K_{fail} is the proportion of three-phase grounded short-circuit faults that cause commutation failure of a DC system, n_{fail} is the number of buses that cause DC commutation failure due to three-phase grounded short-circuit faults, and N_{sum} is the total number of system buses.

2.2. Proportion of DC Power Loss Due to Short-Circuit Faults

The K_{fail} indicator above is a measure of the range of the short-circuit faults that cause a commutation failure in a particular DC system. In addition to focusing on the range of short-circuit faults that cause DC commutation failure, the issue of simultaneous commutation failure of multiple DCs is also of concern to the receiving-end grid operators. In a multi-infeed HVDC transmission system, the inverter stations are coupled to each other through the receiving-end AC system and are electrically close to each other. When the AC system fault is serious or the AC system strength is weak, the commutation failure of one DC system will lead to the continuous commutation failure of multiple DCs and threaten the system power supply reliability of the whole AC-DC hybrid system. Especially for a large-capacity and long-distance HVDC transmission system, it is not easy to recover from a fault, and it is easy to cause great power fluctuations. A commutation failure or DC blocking is enough to destroy the safe and stable operation of the receiving-end grid.

If a bus causes the commutation failure of multiple DCs during a three-phase grounded short-circuit fault, the DC power loss due to the commutation failure is P_{los} MW, defining the severity of the short-circuit fault at that bus as follows:

$$K_{\text{los}} = \frac{P_{\text{los}}}{P_{\text{sum}}} \tag{2}$$

where K_{los} is the proportion of DC power loss caused by a three-phase grounded short-circuit fault at a bus, P_{los} is the amount of DC power loss caused by a three-phase grounded short-circuit fault at the bus, and P_{sum} indicates all the external DC power accepted by the grid.

2.3. Ratio of Lost Energy to Maximum Allowable Released Kinetic Energy

The proportion of DC power loss due to a short-circuit fault is used to analyze the severity of commutation failure from the power perspective. In addition to the size of the power loss, the duration of commutation failure is also a matter of concern. For an HVDC system, if the commutation failure occurs under a short-circuit fault and cannot be recovered to the rated power in a long time, it will undoubtedly have a huge impact on the voltage stability and frequency stability of the AC system. To take into account the impact of DC commutation failure duration, the lost energy calculation method is given here from the energy perspective, so that the impact of DC commutation failure can be measured from both power and duration aspects. The power curves of the DC system during commutation failure and the recovery process are shown in Figure 1. In Figure 1, it is assumed that the DC power initially runs at P_0, and when the commutation failure occurs, the DC power drops to 0. The duration of the commutation failure is T_{F}, after which the DC power starts to recover and the recovery time lasts for T_{R}. Then, the energy loss of this DC commutation failure is defined as:

$$E_{\text{lack}}^{i} = \int_{0}^{T_{\text{F}}+T_{\text{R}}} [P_0 - P_{\text{dc}}(t)]dt \tag{3}$$

where E_{lack}^{i} is the DC i commutation failure power loss and $P_{\text{dc}}(t)$ is the DC power as a function of time.

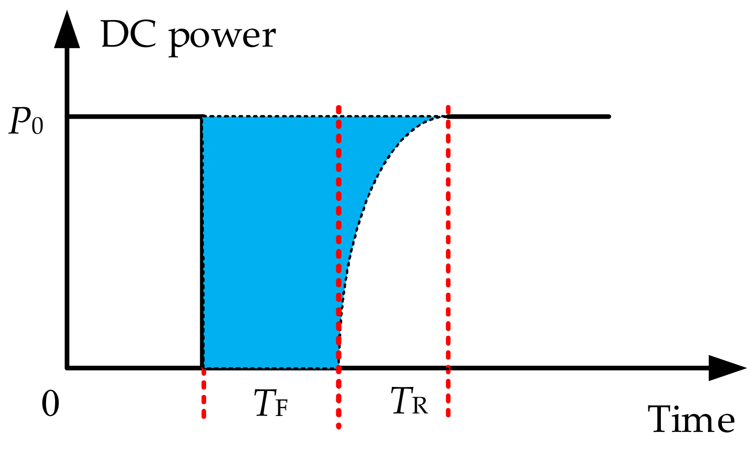

Figure 1. Diagram of energy loss due to the commutation failure.

For a receiving-end grid with multi-infeed HVDC, a single short-circuit fault usually results in the simultaneous commutation failure of multiple DCs. Therefore, for a short-circuit fault at node j, the energy loss caused by it should be the sum of the energy loss of each DC commutation failure, as shown in the following equation:

$$E_{\mathrm{B}}^{j} = \sum_{i \in j} E_{\mathrm{lack}}^{i} \tag{4}$$

where E_{B}^{j} denotes the energy loss of the system caused by a short-circuit fault at node j, and $i \in j$ denotes that a short-circuit fault at node j will cause a DC i commutation failure.

The magnitude of the energy loss shown in Equation (4) can reflect the severity of the commutation failure occurring in the system: the larger the E_{B}^{j}, the greater the energy impact on the system. However, with the same magnitude of energy loss, the threat to the large-scale power system is much smaller than that to the small-scale power system. As an absolute quantity, the magnitude of E_{B}^{j} does not intuitively reflect the relationship between the energy loss and the system scale. Therefore, the following indicator is used as a substitute for the energy loss:

$$K_{\mathrm{eg}} = \frac{E_{\mathrm{B}}^{j}}{\sum\limits_{i=1}^{N_{\mathrm{g}}} W_{\mathrm{eg}}^{i}} \tag{5}$$

where K_{eg} is the ratio of lost energy to maximum allowable released kinetic energy, N_{g} is the number of units, and W_{eg}^{i} is the maximum allowable released rotor kinetic energy of unit i, calculated as follows:

$$W_{\mathrm{eg}}^{i} = \frac{1}{2} J_i \left(\omega_0^2 - \omega_{\mathrm{min}}^2 \right) \tag{6}$$

where J_i is the rotational inertia of unit i, ω_0 is the rated angular speed, and ω_{min} is the allowable minimum angular speed.

2.4. Comprehensive Evaluation for Voltage Stability of Commutation Buses in Multi-Infeed HVDC Systems

The calculation results of different indicators vary greatly in units as well as in values. Therefore, when combining various indicators for analysis, the calculation results of the indicators should be normalized first. The larger the calculation result of the above three indicators, the worse the security and stability of the corresponding aspect; therefore, the following normalization formula is adopted:

$$r_{ij} = \frac{R_{\mathrm{max}}^{j} - R_{ij}}{R_{\mathrm{max}}^{j} - R_{\mathrm{min}}^{j}} \tag{7}$$

where R_{max}^{j} is the upper limit of the allowable values of indicator j in the system, R_{min}^{j} is the lower limit of the allowable values of indicator j in the system, R_{ij} denotes the calculated result of indicator j under object i, and r_{ij} is the normalized result of R_{ij}.

After normalization, the voltage stability of commutation buses of the current system can be evaluated using the comprehensive weight coefficient method in the following way:

$$s = \sum\nolimits_{j=1}^{3} w_j e_j \tag{8}$$

where s is the result of the evaluation for voltage stability of commutation buses and takes a value in the range of 0 to 1. The closer the value is to 1 indicates that the system is more prone to instability due to DC commutation failure; w_j is the weight coefficient of the jth indicator and e_j is the value of the jth indicator of the system, calculated as follows:

$$\begin{cases} e_1 = \max\left\{K^i_{\text{fail}}\right\} \\ e_2 = \max\left\{K^i_{\text{los}}\right\} \\ e_3 = \max\left\{K^i_{\text{eg}}\right\} \end{cases} \tag{9}$$

For the weight coefficient w, the following entropy method is used for calculation. The entropy method is an empowerment method to determine the weight according to the dispersion degree of the indicator value. The greater the dispersion degree of the indicator value, the greater the entropy, and the more useful the information. The indicator should then be assigned a larger weight, and vice versa. The specific weighting steps of the entropy method are as follows:

1. For m feasible solutions, the normalized results of n indicators are calculated while all equipment parameters have been determined.
2. The entropy value of each indicator is calculated as:

$$D_j = -\frac{1}{\ln n}\sum_{i=1}^{m} q_{ij}\ln(q_{ij}) \tag{10}$$

$$q_{ij} = \frac{r_{ij}}{\sum\limits_{i=1}^{m} r_{ij}} \tag{11}$$

   where r_{ij} is the normalized result of the jth indicator under object i.
3. The target coefficient for the jth indicator is calculated as:

$$w''_j = \frac{(1 - D_j)}{\sum\limits_{k=1}^{n}(1 - D_k)} \tag{12}$$

4. Finally, the calculation of the comprehensive weight coefficients is conducted. To make the comprehensive weights as unbiased as possible to either of the subjective and objective weights, the minimum discrimination information principle is used to build an optimization model to determine the comprehensive weights, as follows:

$$\begin{cases} \min J(w) = \sum_{j=1}^{n}\left(w_j \ln\frac{w_j}{w\prime_j} + w_j \ln\frac{w_j}{w''_j}\right) \\ \text{s. t.} \sum_{j=1}^{n} w_j = 1, w_j \geq 0 \end{cases} \tag{13}$$

   where $\boldsymbol{w}$ is a vector consisting of the comprehensive weight coefficients of each indicator and w_j is the comprehensive weight coefficient of indicator j.

By solving the above equation, the final expression for the comprehensive weight coefficient can be obtained as follows:

$$w_j = \frac{\sqrt{w\prime_j w''_j}}{\sum_{i=1}^{n}\sqrt{w\prime_i w''_i}} \tag{14}$$

3. RPCC Method Based on Dynamic Reactive Power Compensation Device

Dynamic reactive power compensation devices are usually added to meet the reactive power demand of the system, such as SVCs, STATCOMs, and synchronous condensers, in the receiving-end grid with multi-infeed HVDC. It is beneficial to suppress the commutation failure of the receiving-end grid with multi-infeed HVDC by reasonably setting the control strategy of dynamic reactive power compensation devices. An RPCC method to help DC commutation failure recovery is provided below.

3.1. Evaluation of the Impact of Dynamic Reactive Power Compensation Devices on Commutation Failure

Before setting up a dynamic reactive power control strategy, it is necessary to define the coupling degree between the dynamic reactive power compensation device and the LCC commutation bus, to determine which dynamic reactive power compensation resources should be invoked in the case of commutation failure of an LCC. To quantitatively analyze the impact of the dynamic reactive power compensation device on the dynamic characteristics of the LCC, this paper uses the voltage interaction factor (VIF), which is defined as follows:

$$\mathrm{VIF}_{ij} = \frac{\Delta U_j}{\Delta U_i} \tag{15}$$

where VIF_{ij} is the VIF of node i to node j, ΔU_j is the voltage change in node j, and ΔU_i is the voltage change in node i. Assuming that there are two nodes numbered i and j in the system when node i puts in a symmetrical three-phase reactor causing the voltage drop on this bus to be ΔU_i, the voltage change in node j is ΔU_j. VIF_{ij} is used as a measure of the voltage interaction between the two buses, which is based on the actual grid model and calculated using time-domain simulation, and the obtained result is more reasonable than the voltage coupling coefficient determined using the AC Thevenin equivalent impedance and the bus-to-bus coupling impedance.

Here, VIF_{ij} is used to characterize the degree of voltage coupling between the reactive power compensation device and the LCC-HVDC drop point, and the value of VIF_{ij} is between 0 and 1. If VIF_{ij} is small and close to 0, it means that the electrical distance between bus i and bus j is far, and the reactive power change at bus i has little impact on bus j voltage. If VIF_{ij} is large and close to 1, it means that the electrical distance between bus i and bus j is close, and the reactive power change at bus i will also have a greater impact on the bus j voltage. Only when the value of VIF_{ij} is greater than a certain threshold is it considered feasible to use the reactive power compensation device at bus i to improve the voltage characteristics of bus j. It should be noted that even if the value of VIF_{ij} is close to 1, it does not mean that the dynamic reactive power compensation device at bus i can necessarily improve the LCC-HVDC recovery characteristics at bus j because the capacity of the compensation device and the LCC-HVDC system also needs to be taken into account. If the capacity of the reactive power compensation device is too small and the output reactive power is limited, then it is also difficult to improve the LCC operating characteristics.

It is worth noting that VIF can only make an initial screening of the devices involved in coordinated reactive power control in terms of the grid structure. For a given reactive power compensation device, even a large VIF value does not necessarily mean that the operating characteristics of the LCC can be improved by a reasonable reactive power control, and the limitations of the reactive power capacity have to be considered. Therefore, the indicator reactive power regulation factor τ is further defined to measure the impact of the output reactive power of the reactive power compensation device on its nodes.

$$\tau^i = \frac{Q^i_{\max} - Q^i_0}{S^i_{\mathrm{short}}} \tag{16}$$

where $Q^i_{\max}$ is the maximum reactive power that can be output by the reactive power compensation device, Q^i_0 is the initial reactive power of the reactive power compensation device, and S^i_{short} is the short-circuit capacity of the access point of the reactive power compensation device.

Using Equations (15) and (16), the impact of the dynamic reactive power compensation device on the commutation failure of the LCC can be evaluated in two ways. If the VIF is small, it means that the dynamic reactive power compensation device is far away from the LCC access point; therefore, it is difficult for the device to play a role in improving the commutation failure no matter how its reactive power is changed. If the reactive power regulation factor τ is small, it means that the dynamic reactive power compensation device has insufficient capacity to regulate the voltage of its access node, let alone regulate the LCC commutation failure. Therefore, for a specified dynamic reactive power compensation device i, participation in suppressing the LCC_j commutation failure requires the following conditions to be met:

$$\begin{cases} VIF_{ij} \geq VIF_C \\ \tau^i \geq \tau_C \end{cases} \quad (17)$$

where VIF_C is the critical value of the voltage interaction factor and τ_C is the critical value of the reactive power regulation factor.

3.2. RPCC Strategy

The corresponding relationship between dynamic reactive power compensation devices and LCCs is filtered based on the results of the evaluation of the impact of dynamic reactive power compensation devices on commutation failure. A dynamic reactive power compensation device can have a corresponding relationship with multiple LCCs, and conversely, an LCC can also have multiple strongly correlated dynamic reactive power compensation devices. The dynamic reactive power compensation device activates the RPCC strategy after a commutation failure with its strongly correlated LCC to assist in voltage recovery of the LCC commutation bus and improve the LCC commutation failure recovery characteristics. According to the response characteristics and distribution of the dynamic reactive power compensation device, the following control principles are given:

1. When the system is at the steady-state point, the reactive power compensation should be mainly based on static reactive power compensation devices and minimize the output reactive power of dynamic reactive power compensation devices to avoid the waste of dynamic reactive power compensation device capacity.
2. For any dynamic reactive power compensation device, the local reactive power or voltage is the control target if no commutation failure occurs with its strongly related LCC.
3. For any dynamic reactive power compensation device, if a commutation failure occurs with its strongly related LCC, the device provides reactive power support as far as possible within its own capacity and bus voltage allowances to help the commutation bus voltage recovery.

The above goal is achieved via auxiliary control signals to the dynamic reactive power compensation device. In general, dynamic reactive power compensation devices can be divided into two categories according to the control objectives, namely, fixed voltage reactive power compensation devices and fixed power reactive power compensation devices, both of which can have auxiliary controllers with the structure shown in Figure 2.

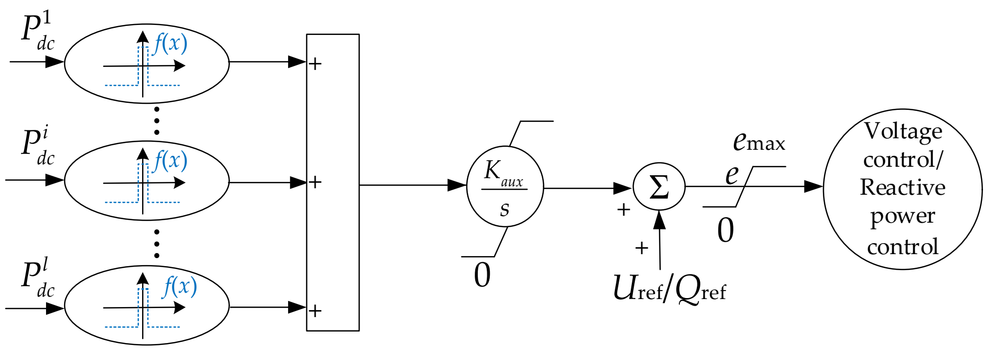

Figure 2. Diagram of the auxiliary control strategy for the dynamic reactive power compensation device.

In Figure 2, the auxiliary controller determines whether a commutation failure occurs in the DC systems based on whether the DC power drops down to near 0. Assuming that there are l DC systems strongly related to the fixed voltage dynamic reactive power compensation device, if no commutation failure occurs in these DC systems, the DC power is maintained at a high value, and after a subsection function (18), the input of the integral link is -1. Since the input of the integral link is negative, the output of the integral link is 0 under the action of the soft limiting link. If any commutation failure occurs in these DC systems after the subsection function (18), the input of the auxiliary controller is not 0 and the auxiliary controller starts to act, attaching a signal to the original voltage or reactive reference value and sending it out to the voltage or reactive controller after the limiting link.

$$f(x) = \begin{cases} 1, & -\varepsilon \leq x \leq \varepsilon \\ -1, & x < -\varepsilon, x > \varepsilon \end{cases} \tag{18}$$

The purpose of the signal limiting $e_{\max}$ is to avoid overvoltage at its node when the dynamic reactive power compensation device provides reactive power support to the LCC converter bus. In the case of fixed-voltage controlled reactive power compensation devices, the control signal limiting $e_{\max}$ directly selects the maximum allowed voltage amplitude. However, in the case of fixed reactive power controlled compensation devices, the relationship between reactive power and voltage amplitude is not clear; therefore, the $e_{\max}$ is adjusted in real time using the following equation:

$$e_{\max} = \min[Q_{\max}, e + K_e(U_{\max} - U)] \tag{19}$$

where $Q_{\max}$ is the maximum reactive power that can be output by the dynamic reactive power compensation device, U is the bus voltage of the dynamic reactive power compensation device, and K_e is the coefficient.

4. Examples

In this section, the analysis is based on the 2025 Jiangsu power grid planning data to verify the effectiveness of the proposed method. According to the 14th Five-Year Plan of Jiangsu Power Grid, the installed capacity of synchronous machines in Jiangsu province will reach 128,000 MW in 2025, and the installed scale of wind power will reach about 30,000 MW. In addition, Jiangsu province will consume up to 39,000 MW of foreign power through HVDC projects. The situation of Jiangsu's power grid receiving foreign power through HVDC systems is shown in Figure 3.

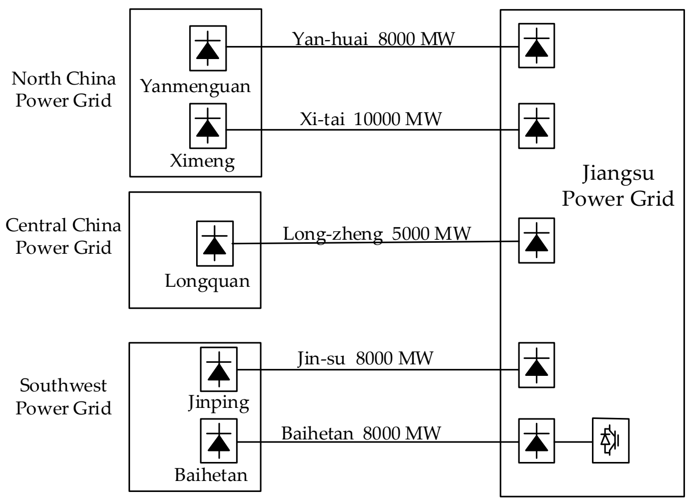

Figure 3. Diagram of HVDC systems in the Jiangsu power grid.

4.1. Evaluation for Voltage Stability of Commutation Buses in Multi-Infeed HVDC Systems in the Jiangsu Power Grid

Firstly, the proportion of short-circuit faults causing each DC commutation failure is calculated according to Equation (1) and only the three-phase grounded short-circuit faults of the 500 kV/1000 kV bus are considered in the calculation. The results are shown in the following Table 1:

Table 1. The proportion of short-circuit faults causing commutation failures in the HVDC system.

HVDC System	The Proportion of Short-Circuit Faults (%)
High-voltage side of Xi-tai	53.47
Low-voltage side of Xi-tai	48.35
Yan-huai	41.42
Baihetan	39.41
Jin-su	28.77
Long-zheng	21.32

According to the calculation results, it can be seen that the proportion of short-circuit faults causing commutation failure on the high-voltage side of the Xi-tai HVDC system is the largest, which can reach up to 50%, and the smallest is the Long-zheng HVDC system. Therefore, with the same probability of short-circuit faults at each bus of the 500 kV grid, the probability of commutation failure at the Xi-tai HVDC system is the largest and the probability of commutation failure at the Long-zheng HVDC system is the smallest.

Then, we calculated the proportion of DC power loss caused by three-phase short-circuit faults at each bus according to Equation (2) and identified the bus that causes the most severe DC power loss as follows:

As can be seen from Table 2, in Jiangsu province, the most serious simultaneous commutation failures of multiple DCs caused by bus short-circuit faults are found in the Suzhou area, including the buses of Sumeili, Sumudu, Suwangyu, Suyuexi, and Sukunnan. For example, when a metallic three-phase grounded short-circuit fault occurs on the Su Meili 500 kV bus, four DCs, including Jin-su, Baihetan, Xi-tai, and Long-zheng, will cause a commutation failure.

Table 2. The proportion of DC power loss caused by three-phase short-circuit faults.

Faulted Bus	The Proportion of DC Power Loss (%)
Sumudu 51	51.52
Suyushan 51	47.85
Sukunnan 51	44.75
Sushipai 51	44.75
Suwunan 51	44.75
Suchefang51	41.54
Sumeili 51	41.54
Suwangyu 51	41.54
Suxinan 51	41.54
Suyuexi 51	41.54

Assuming that the maximum allowable frequency deviation of the system is −0.2 Hz, the maximum allowable released rotor kinetic energy of the system can be calculated as 5922 MJ according to Equation (6). Then, the ratio of lost energy for the commutation failure to the maximum allowable released kinetic energy under each bus short-circuit fault is calculated according to Equation (5), and the bus that causes the most serious energy loss in the DC commutation failure is listed as follows:

From the calculation results in Table 3, it can be seen that the problem of lost energy caused by commutation failure due to bus short-circuit fault is the most serious in the Suzhou area. Comparing Tables 2 and 3, it can be seen that the fault ranking causing energy loss and power loss is not the same. This is because some faults may cause simultaneous commutation failure of multiple DCs, but if the DCs can recover from the commutation failure quickly, then the lost energy caused by the commutation failure is not so serious. Some faults may cause multiple commutation failures in the same DC, thus making the DC system unable to recover from the commutation failures for a long time and eventually leading to an increase in the lost energy of the system.

Table 3. The ratio of lost energy to maximum allowable released kinetic energy.

Faulted Bus	The Ratio of Lost Energy to Maximum Allowable Released Kinetic Energy (%)
Sumudu 51	49.98
Suyushan 51	49.39
Sukunnan 51	44.81
Sushipai 51	43.94
Suwunan 51	43.86
Suchefang51	43.67
Sumeili 51	42.84
Suwangyu 51	40.66
Suxinan 51	40.24
Suyuexi 51	39.58

Finally, six typical operation modes of the Jiangsu power grid, including summer peak, summer valley, winter peak, winter valley, flood peak, and flood valley, were selected to calculate the comprehensive evaluation indicators for the voltage stability of commutation buses in multi-infeed HVDC systems under different operation modes. The results are obtained as shown in Table 4.

Table 4. Comprehensive evaluation results of voltage stability of commutation buses under different operation conditions.

Operation Mode	Comprehensive Evaluation Indicator s
Summer peak	0.51
Flood valley	0.45
Flood peak	0.41
Winter peak	0.36
Summer valley	0.32
Winter valley	0.31

In Table 4, the closer the comprehensive evaluation indicator s is to 1, the more the system is threatened by the DC system commutation failure, and the more detrimental it is to the safe and stable operation of the system. As can be seen from Table 4, the highest comprehensive evaluation indicator is the summer peak, when the HVDC systems are basically in a full delivery state and heavily loaded, so that multiple HVDC systems cannot recover quickly from a commutation failure after the fault is cleared, which increases the lost energy. In addition to the summer peak, the system is most threatened by the commutation failure under the flood valley operation mode, which is because the HVDC systems are basically in full delivery; however, due to the light load, a large number of units within the Jiangsu power grid are not turned on, which reduces the system strength and expands the impact of commutation failure.

4.2. RPCC Method Verification

Various dynamic reactive power compensation devices are now available in the south of Jiangsu, including the Meili-Mudu UPFC, the Wujiangbian STATCOM, and the condenser at the Jin-su HVDC commutation bus. Moreover, three types of dynamic reactive power compensation devices, including the condenser, STATCOM, and UPFC, will soon exist in the Suzhou area and all of them can continuously and quickly control the bus voltage and provide RPCC for the system after a fault, which is beneficial to improve the voltage stability and anti-interference capability of the system and improve the recovery characteristics. The application effect of the proposed RPCC method is verified in each of the three dynamic reactive power compensation devices mentioned above.

4.2.1. The Effect of the RPCC Strategy Applied to the Suzhou Condenser

The Suzhou condenser is located near the Jin-su HVDC inverter station to ensure the safe and stable operation of the Jin-su HVDC. However, according to the evaluation results of Equations (15) and (16), the Suzhou condenser can also play an improving role in the LCC on the high voltage side of the Baihetan HVDC inverter station. The following example verifies the effect of the RPCC method applied in the Suzhou condenser on the LCC of Baihetan. When a short-circuit fault occurred near the 500 kV bus Guotaizhou, a comparison of the reactive power output of the Suzhou condenser with and without applying the proposed RPCC strategy was produced and is shown in the following Figure 4:

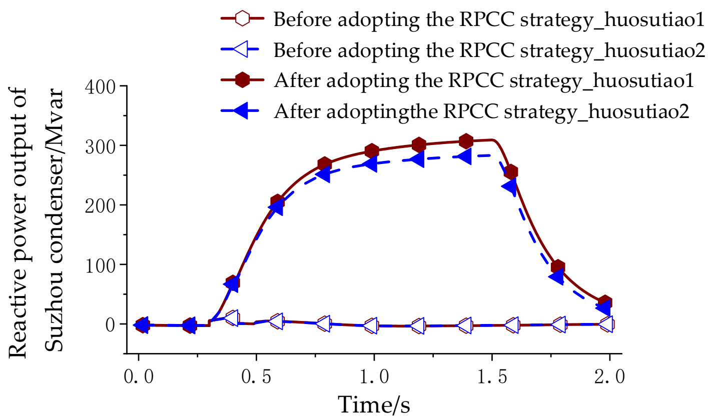

Figure 4. The reactive power output of the Suzhou condenser during a bus short-circuit fault at Guotaizhou.

The DC voltage of the LCC of the Baihetan HVDC system before and after adopting the RPCC strategy is shown in the following Figure 5:

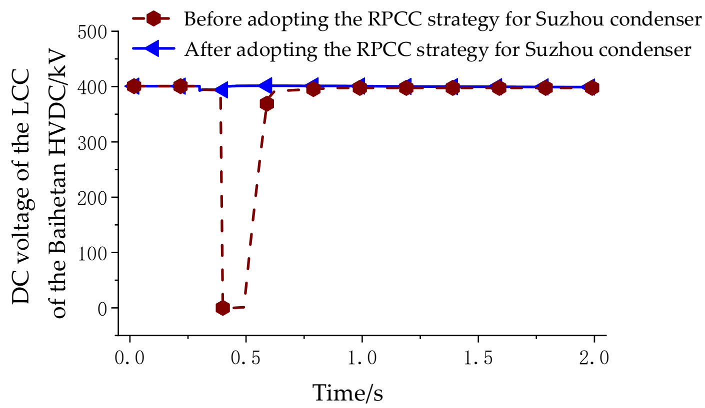

Figure 5. The DC voltage of the LCC of the Baihetan HVDC system during a bus short-circuit fault at Guotaizhou.

It can be seen that after applying the proposed RPCC strategy, the reactive power output of the Suzhou condenser increases significantly during the fault and recovery process. Under certain critical faults, this change may prevent commutation failure in the Baihetan HVDC system.

4.2.2. The Effect of the RPCC Strategy Applied to the Wujiangbian STATCOM

According to the evaluation results of Equations (15) and (16), the Wujiangbian STATCOM can provide voltage support to the Jin-su HVDC commutation bus. By adjusting the AC voltage reference value U_{ref} of Wujiangbian STATCOM according to the proposed control strategy and applying a short-circuit fault near the Guotaizhou 500 kV bus, a comparison of the reactive power output of Wujiangbian STATCOM with and without applying the proposed RPCC strategy was produced and is shown in the following Figure 6:

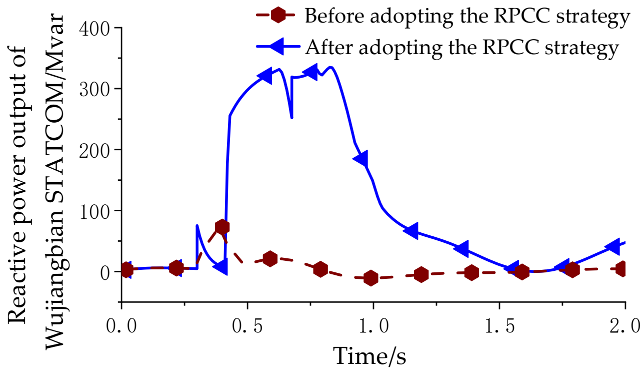

Figure 6. The reactive power output of Wujiangbian STATCOM during a bus short-circuit fault at Guotaizhou.

The DC voltage of the LCC of the Jin-su HVDC system before and after adopting the RPCC strategy is shown in the following Figure 7:

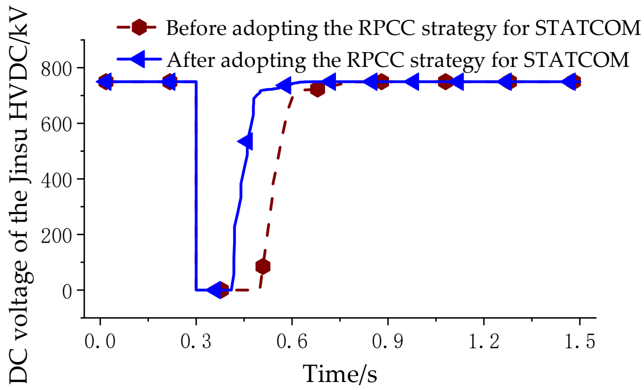

Figure 7. The DC voltage of the Jinsu HVDC system during a bus short-circuit fault at Guotaizhou.

It can be seen that after applying the RPCC strategy proposed in this paper, the reactive power output of the Wujiangbian STATCOM increases significantly during faults and recovery. Under some faults, this change can significantly reduce the duration of commutation failure of the Jin-su HVDC system. According to the simulation results in Figure 7, the commutation failure duration of the Jin-su HVDC system is reduced from 200 ms to 100 ms, thus reducing the lost energy of the system.

4.2.3. The Effect of the RPCC Strategy Applied to the Suzhou UPFC

According to the evaluation results of Equations (15) and (16), the parallel side of the Suzhou UPFC can also provide voltage support to the Jin-su HVDC system commutation bus. By adjusting the AC voltage reference value U_{ref} on the parallel side of the Suzhou UPFC according to the proposed control strategy and applying a short-circuit fault at the Suquanfu 500 kV bus, a comparison of the reactive power output on the parallel side of the Suzhou UPFC with and without applying the proposed RPCC strategy was produced and is shown in the following Figure 8:

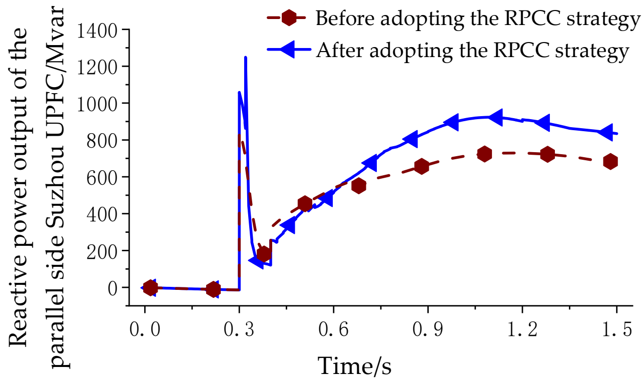

Figure 8. The reactive power output of the parallel side Suzhou UPFC during a bus short-circuit fault at Suquanfu.

The DC voltage of the LCC of the Jin-su HVDC system before and after adopting the RPCC strategy is shown in the following Figure 9:

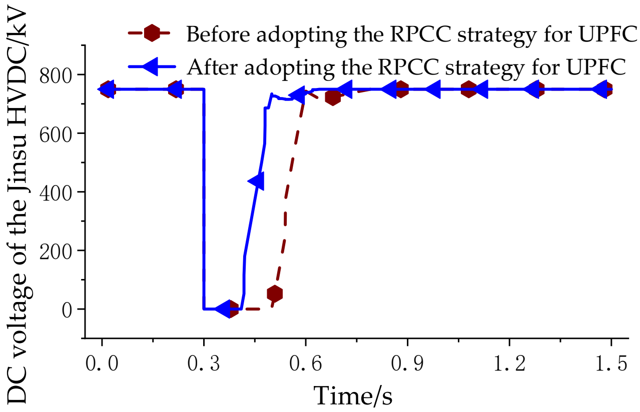

Figure 9. The DC voltage of the Jinsu HVDC system during a bus short-circuit fault at Suquanfu.

It can be seen that after applying the RPCC strategy proposed in this paper, the reactive power output on the parallel side of the UPFC increases significantly during the fault and the recovery process, thus suppressing the Jin-su HVDC system commutation failure, which is mainly reflected in the significant reduction in the Jin-su HVDC commutation failure duration under some faults. According to the simulation results in Figure 9, the commutation failure duration of the Jin-su HVDC system is reduced from 200 ms to 100 ms, thus reducing the lost energy of the system.

Table 5 shows the commutation failure duration in Figures 5, 7 and 9 before and after applying the RPCC strategy. It can be seen that after applying the RPCC strategy, the duration of commutation failure in the HVDC system is significantly reduced; under certain critical faults, this change may prevent commutation failure of the HVDC system. Therefore, the proposed RPCC method can effectively improve the commutation failure problem in some HVDC systems.

Table 5. The commutation failure duration before and after applying the RPCC strategy.

Faulted Bus	HVDC System	Commutation Failure Duration before Applying the RPCC Strategy (ms)	Commutation Failure Duration after Applying the RPCC Strategy (ms)
Guotaizhou	Baihetan	100	0
Guotaizhou	Jin-su	200	100
Suquanfu	Jin-su	200	100

5. Conclusions

This paper proposes a method for evaluating the voltage stability of commutation buses in multi-infeed HVDC systems and an RPCC method suitable for receiving-end power grids with high DC power penetration. Three indicators are used to characterize the degree of system impact from different aspects in the evaluation method for voltage stability of commutation buses of multiple DCs, namely, the proportion of short-circuit faults causing DC commutation failure, the proportion of DC power loss due to short-circuit faults, and the ratio of lost energy to maximum allowable released kinetic energy. A comprehensive evaluation method is proposed based on the entropy weight method. The RPCC method first evaluates the impact of the dynamic reactive power compensation device on the DC system and then filters the dynamic reactive power compensation devices that can resist the commutation failure of each DC system. The simulation results in the Jiangsu power grid indicate that the proposed method can effectively evaluate the voltage stability of commutation buses in multi-infeed HVDC systems of the Jiangsu power grid, while the RPCC method can effectively improve the commutation failure problem in some DC systems.

Author Contributions: Conceptualization, Y.Y.; methodology, Y.Y. and G.W.; software, Y.Y.; formal analysis, Y.Y.; investigation, Z.Z.; resources, Y.H.; data curation, Y.Z. and J.L.; writing—original draft preparation, Y.Y.; writing—review and editing, Y.H.; visualization, Y.H.; supervision, Z.Z. and G.W.; project administration, Y.Z. and J.L.; funding acquisition, Y.Z. and J.L. All authors have read and agreed to the published version of the manuscript.

Funding: This research was funded by the East China Branch of State Grid Corporation of China, grant number 52080023002P.

Data Availability Statement: Not applicable.

Conflicts of Interest: The authors declare no conflict of interest.

References

1. Huang, D.; Shu, Y.; Ruan, J.; Hu, Y. Ultra High Voltage Transmission in China: Developments, Current Status and Future Prospects. *Proc. IEEE* **2009**, *97*, 555–583. [CrossRef]
2. Rahimi, E.; Gole, A.M.; Davies, J.B.; Fernando, I.T.; Kent, K.L. Commutation Failure in Single- and Multi-Infeed HVDC Systems. In Proceedings of the 8th IEE International Conference on AC and DC Power Transmission, London, UK, 28–31 March 2006; pp. 182–186.
3. Jingbo, H.; Mingjie, L.; Jun, Y.; Qing, C.; Tao, X.; Zhao, Y. Research on Dynamic Characteristics and Countermeasures of AC-DC Hybrid Power System with Large Scale HVDC Transmission. In Proceedings of the 2014 International Conference on Power System Technology, Chengdu, China, 20–22 October 2014; pp. 799–805.
4. Weifang, L.; Yong, T.; Guangquan, B.; Yao, S. Voltage Stability Analysis of Multi-Infeed AC/DC Power System Based on Multi-Infeed Short Circuit Ratio. In Proceedings of the 2010 International Conference on Power System Technology, Hangzhou, China, 24–28 October 2010; pp. 1–6.
5. Zhang, F.; Xin, H.; Wu, D.; Wang, Z.; Gan, D. Assessing Strength of Multi-Infeed LCC-HVDC Systems Using Generalized Short-Circuit Ratio. *IEEE Trans. Power Syst.* **2019**, *34*, 467–480. [CrossRef]
6. Li, Y.; Shi, D.; Chen, J.; Duan, X. Integrated Short Circuit Ratio Strength Index for Static Voltage Stability Analysis of Multi-Infeed LCC-HVDC Systems. *Zhongguo Dianji Gongcheng Xuebao/Proc. Chin. Soc. Electr. Eng.* **2017**, *37*, 6471–6480. [CrossRef]
7. Zhou, H.; Yao, W.; Ai, X.; Li, D.; Wen, J.; Li, C. Comprehensive Review of Commutation Failure in HVDC Transmission Systems. *Electr. Power Syst. Res.* **2022**, *205*, 107768. [CrossRef]
8. Wang, L.; Wang, G.; Li, H.; Li, Z. Risk Evaluation of Commutation Failure in Multi-Infeed HVDC Systems under AC System Fault Conditions. *Dianli Xitong Zidonghua/Autom. Electr. Power Syst.* **2011**, *35*, 9–14.
9. Shao, Y.; Tang, Y. Fast Evaluation of Commutation Failure Risk in Multi-Infeed HVDC Systems. *IEEE Trans. Power Syst.* **2018**, *33*, 646–653. [CrossRef]
10. Xiao, H.; Li, Y.; Gole, A.M.; Duan, X. Computationally Efficient and Accurate Approach for Commutation Failure Risk Areas Identification in Multi-Infeed LCC-HVdc Systems. *IEEE Trans. Power Electron.* **2020**, *35*, 5238–5253. [CrossRef]
11. Chen, N.; Yang, Y.; Li, L.; Cui, C.; Xue, Y.; Zhang, X.-P. Commutation Failure Prediction for Multi-Infeed LCC-HVDC Systems Under Asymmetrical Faults. *IEEE Trans. Power Deliv.* **2023**, *38*, 2034–2046. [CrossRef]
12. Wang, L.; Yao, W.; Xiong, Y.; Shi, Z.; Wen, J. Commutation Failure Analysis and Prevention of UHVDC System with Hierarchical Connection Considering Voltage Harmonics. *IEEE Trans. Power Deliv.* **2022**, *37*, 3142–3154. [CrossRef]

13. Li, X.; Li, F.; Chen, S.; Li, Y.; Zou, Q.; Wu, Z.; Lin, S. An Improved Commutation Prediction Algorithm to Mitigate Commutation Failure in High Voltage Direct Current. *Energies* **2017**, *10*, 1481. [CrossRef]
14. Wang, F.; Liu, T.; Li, X. Decreasing the Frequency of HVDC Commutation Failures Caused by Harmonics. *IET Power Electron.* **2017**, *10*, 215–221. [CrossRef]
15. Xiao, H.; Li, Y.; Duan, X. Enhanced Commutation Failure Predictive Detection Method and Control Strategy in Multi-Infeed LCC-HVDC Systems Considering Voltage Harmonics. *IEEE Trans. Power Syst.* **2021**, *36*, 81–96. [CrossRef]
16. Xiao, H.; Li, Y.; Duan, X. Efficient Approach for Commutation Failure Immunity Level Assessment in Hybrid Multi-Infeed HVDC Systems. *J. Eng.* **2017**, *2017*, 719–723. [CrossRef]
17. Guo, C.; Liu, Y.; Zhao, C.; Wei, X.; Xu, W. Power Component Fault Detection Method and Improved Current Order Limiter Control for Commutation Failure Mitigation in HVDC. *IEEE Trans. Power Deliv.* **2015**, *30*, 1585–1593. [CrossRef]
18. Hansen, A.; Havemann, H. Decreasing the Commutation Failure Frequency in HVDC Transmission Systems. *IEEE Trans. Power Deliv.* **2000**, *15*, 1022–1026. [CrossRef]
19. Wang, Y.; Li, X.; Cai, Z.; Zhao, J.; Guo, Y.; Wang, J. Continuous Commutation Failure Suppression Method Based on Dynamic Compensation of Firing Angle Deviation. *Int. J. Electr. Power Energy Syst.* **2023**, *147*, 108818. [CrossRef]
20. Luo, X.; Li, F.; Fan, L.; Niu, T.; Li, B.; Tian, L.; Yu, H. Influence of Synchronous Condensers on Operation Characteristics of Double-Infeed LCC-HVDCs. *Processes* **2021**, *9*, 1704. [CrossRef]
21. Katsuya, Y.; Mitani, Y.; Tsuji, K. Power System Stabilization by Synchronous Condenser with Fast Excitation Control. In Proceedings of the PowerCon 2000, 2000 International Conference on Power System Technology, Proceedings (Cat. No.00EX409), Perth, Australia, 4–7 December 2000; Volume 3, pp. 1563–1568.
22. Lei, Y.; Li, T.; Tang, Q.; Wang, Y.; Yuan, C.; Yang, X.; Liu, Y. Comparison of UPFC, SVC and STATCOM in Improving Commutation Failure Immunity of LCC-HVDC Systems. *IEEE Access* **2020**, *8*, 135298–135307. [CrossRef]
23. Zhang, Y.; Tang, F.; Qin, F.; Li, Y.; Gao, X.; Du, N. Research on Dynamic Reactive Power Compensation Scheme for Inhibiting Subsequent Commutation Failure of MIDC. *Sustainability* **2021**, *13*, 7829. [CrossRef]
24. Wang, Q.; Li, T.; Tang, X.; Liu, F.; Lei, J. Study on the Site Selection for Synchronous Condenser Responding to Commutation Failures of Multi-Infeed HVDC System. *J. Eng.* **2019**, *2019*, 1413–1418. [CrossRef]
25. Zhang, H.; Liu, F.; Li, W. Site Selection for Dynamic Reactive Power Compensation and Improvement of Recovery from Commutation Failures in Multi-Infeed HVDC System. *Dianli Xitong Zidonghua/Autom. Electr. Power Syst.* **2016**, *40*, 133–138. [CrossRef]